GLOBAL PROPERTIES OF HIGH LIQUID LOADING TURBULENT CRUDE OIL + METHANE/AIR JET DIFFUSION FLAMES

P. Dutta, J. P. Gore, Y. R. Sivathanu and P. E. Sojka
Thermal Sciences and Propulsion Center
School of Mechanical Engineering
Purdue University
West Lafayette, IN 47907

Submitted to: ASME National Heat Transfer Conference
Symposium on Heat Transfer in Fire and Combustion Systems.

Date Submitted: January 1993

Address correspondence to:

J. P. Gore
School of Mechanical Engineering
Purdue University
West Lafayette, IN 47907

GLOBAL PROPERTIES OF HIGH LIQUID LOADING TURBULENT CRUDE OIL + METHANE/AIR JET DIFFUSION FLAMES

P. Dutta, J. P. Gore, Y. R. Sivathanu and P. E. Sojka
Thermal Sciences and Propulsion Center
School of Mechanical Engineering
Purdue University
West Lafayette, IN 47907

ABSTRACT

Measurements of atomization quality, flame heights, radiant loss fractions, and optical properties for Alberta sweet crude-oil/methane flames established on a novel burner for simulating well blowout fires are reported. The results show the effects of two phase flow on flame heights. The measurements of radiant loss fractions and the optical properties suggest that the high momentum at the exit of the present burner reduces the soot loading and the resulting radiation heat loss. The measured high temperatures suggest that almost complete combustion of crude oil is obtained. However, scaleup tests as well as information concerning the physical processes in the present atomizer and burner are essential for the application of the present results to practical fires and combustion devices.

INTRODUCTION

Oil well blowout fires during drilling, production or workover present a serious hazard to personnel, environment and equipment particularly on off-shore platforms (Evans and Pfenning, 1985; Gore and Evans, 1991). Typical oil well blowout fires involve combustion of a mixture of liquid and gaseous fuels. The atomization of the liquid is caused by the expansion of the mixture to atmospheric pressure. Heat transfer from the combustion zone established by the

gaseous components and the fuel vapor in conjunction with the atmospheric oxygen causes evaporation of the atomized liquid fuel. The infrared radiation energy leaving the resulting fires is hazardous to the platform, equipment and personnel.

Typically, material exiting an oil well consists of 80 to 95% liquid with 20 to 5% gases and vapors by mass. In the absence of wind the material expands in a vertical jet configuration, mixes with surrounding air and forms turbulent jet diffusion flames stabilized at or above the well head. As previously observed in blowout fires and more recently in the oil well fires in Kuwait, the liquid atomizes and evaporates effectively in this configuration and flames are stabilized. These jets represent high liquid loading dense sprays that have not been studied in the literature extensively (Faeth, 1987). The mechanisms by which these flames stabilize in spite of the high exit momentum are also not understood.

The flame length, size, and radiation properties of the high liquid loading two phase flames have not received much attention in the literature except the study of Hustad and Sonju (1986), which involved global property measurements for relatively large scale (1-8 MW) oil/gas flames. The oil and gas were mixed in a chamber upstream of large diameter (10 mm - 33 mm) nozzle exit. In such a configuration, the quality of atomization changes with liquid loading and exit diameter. The measurements of visible flame lengths by Hustad and Sonju (1986) showed that the two phase flames

are much longer than gaseous flames with similar heat release rates. However, due to the large size of the flames, information concerning drop sizes and the extent to which the distance needed for the evaporation of the fuel affected the flame lengths could not be obtained.

Laboratory tests of two-phase spray flames have been restricted to relatively low liquid loading since conventional twin fluid atomizers require high kinetic energy of the gas phase for effective atomization. Therefore, liquid mass fraction in the incoming stream has been restricted to 0.5 in past intermediate scale and laboratory scale tests (Gore et al., 1991; Gore and Evans, 1991). Attempts to increase the liquid loading resulted in large drops. Large amount of unburnt crude oil also exited the flame due to lack of efficient evaporation. Therefore, an effervescent atomizer burner was developed for the establishment of high liquid loading crude oil jet flames in the laboratory. The effervescent atomizer concept and design followed the work of Lund et al. (1993). A study of the flames stabilized on this burner is expected to improve the understanding of oil well blowout fires due to the inherent similarity in the atomization and combustion processes.

The objectives of the present paper are: (1) to describe a successful design of the atomizer burner; (2) to discuss global properties (visible flame length, radiative heat flux to surrounding objects) of the crude-oil/methane flames stabilized on

the burner; and (3) to report path integrated measurements of emission temperature and monochromatic transmittance to help understand the behavior of the radiative flux. The present results for the visible flame height are also compared to those of Hustad and Sonju (1986) to highlight the effects of the atomization quality on the flame length.

EXPERIMENTAL METHODS

A sketch of the effervescent atomizer burner is shown in Fig. 1. The effervescent atomization portion of the burner follows the design of Lund et al. (1993) closely. The crude oil flows into an annular space formed by the body of the burner and the central methane injection tube. The methane injection tube is similar to the aeration tube of Lund et al. (1993). In order to stabilize the flame on the burner port, a ring flame established by a small flow of hydrogen is established near the burner orifice. The two phase material exits the central 0.18 mm orifice and flows through the ring flame which helps establish a jet flame attached to the 4.76 mm diameter exit port of the burner. The section containing the exit port is cooled by a small flow of water flowing through an annular space to avoid fuel coking near the orifice.

Figure 2 is a schematic of the flow system used to control the pressures and the mass flow rates of crude oil, methane and hydrogen flowing into the burner. The crude oil is stored in a tank rated for 2 MPa. The liquid in the tank is pressurized using nitrogen connected to the gas space of the tank via a pressure regulator. The pressure in the tank is thus maintained by admitting

nitrogen into the tank as the liquid is used. The liquid flow rate is metered by a Nupro "S" series Fine Metering Valve. A shut-off valve is included so that the metering position can be maintained from one test to another. The flow rate is monitored by a calibrated rotameter. The liquid pressure just upstream of the burner was monitored to be 205 KPag using an Ashcroft pressure gauge for all the tests reported here. The methane gas pressure upstream of the burner has a similar value and is also maintained for all the tests. The mass flow rate of methane is therefore governed by a choked metering valve mounted downstream of a rotameter. The hydrogen flow is also monitored by a rotameter.

Table 1 shows the operating conditions for the flames studied during the present investigation. The mass flow rate of the atomizing methane varied between 5 and 20 % of the mass flow rate of the crude oil. The Alberta sweet crude oil has a density of 816 kg/m^3, viscosity of 5 CP, and surface tension of 30 dynes/cm (Lund et al., 1993). The hydrogen flow used for flame attachment did not affect the atomization quality significantly and was maintained at 16.4 mg/s for all the flames except the last. In order to stabilize the flame with the highest crude oil flow, a higher flow of hydrogen (21.2 mg/s) was required. The heat release rates for the flames varied between 9 and 21 kW based on nominal heating values of 42500 kJ/Kg for the crude oil, 50000 kJ/Kg for methane, and 119000 kJ/Kg for hydrogen. The Reynolds number characteristic of the jet can be evaluated based on the external orifice diameter (4.76 mm) on which the flame is stabilized or based on the diameter

through which the two phase material exits (0.18 mm). The use of the larger diameter assumes that the material expands to fill the exit port while the use of the smaller diameter assumes that the jet is formed independent of the external orifice. The two different assumptions lead to Reynolds number differing by two orders of magnitude. The issue of the appropriate characteristic dimension is not currently resolved as discussed later.

The radiative heat flux distribution from the flames to the surface of a long cylindrical enclosure with a base aligned at the level of the burner (semi-infinite cylindrical enclosure) was measured using a Medtherm wide angle (150°) radiometer. The resulting data were integrated to obtain the total energy radiated by the flames. The radiative fractions obtained from these measurements are listed in Table 1. These vary from approximately 10% for the flames with the highest methane loading to approximately 20% for the flames with the highest crude oil loading. These values are relatively low indicative of highly forced jets. However, measurements of velocities are needed to clarify the issue of momentum vs buoyancy effects further.

The atomizer-burner was operated in an inverted mode in a cold spray configuration to evaluate its performance in terms of drop size distributions. A Malvern 2600 particle size analyzer with a 300 mm focal length was used for these tests similar to previous work (Lund et al. 1993). The particle sizes were measured at a distance of 25 diameters downstream of the atomizer to ensure that

most of the particles are spherical drops. Effects of total oil flow rate and of the methane to oil mass flow rate ratio on the drop size distribution were studied.

The flames were stabilized with the burner facing vertically up. Past tests by Lund et al. (1993) have shown that the orientation does not affect the atomization quality. The vertically-up orientation is clearly preferred for the removal of the exhaust products as well as for simulating the actual oil well fires. A VHS video camera with 1/1000 s exposure time was used to obtain a video record of the jet flames. Several frames of this record were used to obtain the mean visible flame height for the different operating conditions. The surface of the enclosure in which the burner was mounted was examined for the deposition of unburnt oil and none was found. Metal strips inserted into the post flame region also did not show deposits of unburnt oil or soot particles suggesting that the atomizer-burner is operating in a qualitatively satisfactory manner.

In order to examine the emission of smoke into the exhaust stream as well as understand the radiative heat loads from the different flames, measurements of path integrated transmittance and path integrated emission temperatures were obtained for diametric paths at various heights above the burner exit. The instrumentation used for these tests was developed by Sivathanu et al. (1991). However, instead of inserting the purged stainless steel probes into the flame, the entire flame was observed to obtain path

integrated absorption and emission data.

A helium neon laser (632.8 nm wavelength) with a chopper was used to obtain the monochromatic transmittance of the flames. The transmittance of the flames is lower than unity due to absorption by soot particles and intermediate hudrocarbon species as well as scattering and absorption by the liquid oil drops along the path. In the parts of the flame that contribute to significant flame radiation, the reduction in the transmittance is dominated by absorption due to soot particles. Emission at 900 and 1000 nm is measured by two calibrated photomultiplier tubes with narrow band optical filters mounted in front. The emission data are used to infer the temperature assuming specific absorption coefficients of soot particles given by Dalzell and Sarofim (1969). These values have been found satisfactory for obtaining emission temperature data (Sivathanu et al., 1993). Possible interference from emission by hydrocarbon species other than soot particles was neglected as a first step.

RESULTS AND DISCUSSION

Figure 3 shows the distribution of drop sizes measured by the Malvern analyzer at an axial location of x/d = 25 along the centerline of the spray for three different liquid flow rates with a fixed methane to liquid flow rate ratio. The Sauter mean diameter (SMD), which is significant in determining the evaporation rates, increases with the liquid flow rate between 260 mg/s and 360 mg/s but appears to stay almost constant between 360 mg/s and 400 mg/s. The resulting changes in evaporation length for the liquid drops

may translate into differences in the visible flame heights as will be seen later.

It was observed before (Lund et al., 1993) that the ratio of the methane to oil mass flow rates may affect the drop size more significantly than the total liquid flow rate. Figure 4 shows the drop size distribution measured by the Malvern analyzer for a fixed heat release rate of the flame (Q_f = 14 kW) and varying methane to oil mass ratios. For a mass ratio of 5% methane, the drops have an SMD of 38.69 microns. This decreases to 26.93 microns as the methane flow rate is increased to 10% and then to 23.66 microns as the methane flow rate increase further to 14%. It is therefore expected that the flame height will increase with decreasing methane to oil ratio.

Figure 5 shows the flame height "H_f" normalized by the external orifice diameter "d" (4.76 mm) plotted as a function of total heat release rate for the first seven flames in Table 1. The last flame had a higher flow of hydrogen for stabilization and hence is not considered together with the others. As seen in Fig. 5, the flames are taller for lower methane loading. For the methane loading of 5%, the flame height increases with heat release rates. This is probably due to the longer evaporation time needed first because of the higher mass flow rate of oil and second because of the larger drop size produced at higher liquid flow rates. The height of buoyant jet flames also increases with heat release rate due to the slower relative air entrainment rates with the

decreasing influence of buoyancy. Depending up on which one of the two characteristic diameters is appropriate the present flames would be in the buoyant or forced jet regimes. Measurements of velocities at the exit would clarify this question. However, whether larger evaporation length affects flame lengths can be assessed by fixing the heat release rate and varying the liquid loading.

Figure 6 shows that for a fixed heat release rate of 14 kW, the flame height normalized by the external orifice diameter decreases with increasing methane to crude oil mass flow rate ratio. This is in agreement with the smaller drops created by the larger atomization flow rate leading to a shorter evaporation length. It also suggests that the changes in flame length with heat release rates are partly due to two phase flow effects unique to spray flames.

The flame heights discussed above are plotted as a function of Froude number in Fig. 7 together with previous data for gaseous flames from Sivathanu (1990) and the correlations of Hustad and Sonju (1985) for methane and propane gaseous jet flames. The Froude number has not been modified by the two phase flow correction suggested by Hustad and Sonju (1985). However, the velocity and the diameter used in Fig. 7 is based on the two phase density and the total mass flow rate exiting the external orifice. On the log scale of the plot, the two phase flame data appear to be in agreement with the correlations. Actually as seen from the two previous

figures, systematic variation of 20 to 40 % exists based on the evaporation length requirements for the different conditions. The flame lengths for two phase jets measured by Hustad and Sonju (1985) agree with the correlation only when a two-phase flow modification is made to the Froude number. For some conditions, the two-phase flow modification alters the Froude numbers by an order of magnitude. This behavior is indicative of the differences in atomization quality affecting the lengths of spray flames.

The radiative heat flux to a semi-infinite cylinder surrounding the flames was measured using a wide angle radiometer. The distance of the radiometer from the flame axis during the axial traverse was selected to be equal to the flame height H_f based on the scaling rule devised by Sivathanu and Gore (1993). The radiative heat flux was normalized by the total radiant output of the flame divided by the surface area of an imaginary sphere with radius equal to the distance of the detector from the flame axis. The normalized heat flux plotted as a function of the normalized axial distance is shown in Fig. 8. The data for the eight flames collapse extremely well on the plot of Fig. 8 suggesting that the radiation scaling of Sivathanu and Gore (1993) is applicable to two phase flames. The effects of different fuel properties (soot concentrations and temperature) are accounted for by the radiation fraction used in the scaling. The differences in geometry of the flame are accounted by the use of the flame height. Therefore, effects of the two phase flow are built into the scaling via the effects on flame length caused by different evaporation length

requirements. As pointed out by Sivathanu and Gore (1993) the collapse of Fig. 8 provides a convenient method for obtaining the total radiant output of a jet flame by making the radiation heat flux measurement at a single point.

As described in Table 1, the radiative heat loss fractions, X_R, vary between 10.2 % and 21.4 %. As expected, X_R increases with decreasing methane loading due to the propensity of crude oil flames to soot. The values of X_R are lower than expected. For buoyant methane jet flames X_R of approximately 18% is reported in the literature (see Faeth et al., 1989, and their references), for pool flames burning Alberta sweet crude oil a value of X_R=30% has been reported (Gore et al., 1991). Thus the values of X_R for the present jet flames are unexpectedly low. Such low values can be realized if the flame temperatures are low due to incompleteness of combustion or if the sooting tendency of crude oil is substantially diminished in the present flame configuration. These questions can be discussed with the help of the emission and absorption data.

Figure 10 shows the measurements of emission temperature and transmittance for flames with three methane to oil mass flow rate ratios. The heat release rate is maintained at 14 kW for all cases. Since the measurements are path integrated, the temperature probe selects the peak values along the path. For the highest methane loading the peak temperatures are approximately 2200 K near the injector exit and reduce to approximately 2150 K at approximately x/d=70 before decreasing beyond the flame tip. The small decrease

in flame temperature is due to the relatively low radiative heat loss. The high peak temperatures represent almost complete combustion of the fuel. With increasing liquid loading, the peak temperatures decrease only slightly near the burner exit. For the lowest methane loading, the temperatures decrease by approximately 300 K with axial distance primarily due to radiative heat loss. Naturally, soot oxidation reactions are slowed down due to this decrease in temperature. Thus the highest liquid loading flame shows emission due to soot until x/d=120. The reduction in temperature nullifies some of the expected increase in radiant output with higher liquid loading.

The increase in flame emissivity, characterized by the decrease in transmittance of the diametric path, is also shown in Fig. 10. The transmittance for the highest liquid loading flame decreases to approximately 0.6 while that for the intermediate and low liquid loading cases is much higher. The overall decrease in transmittance causes the total radiant energy for the high liquid loading flame to increase from 10.2 % to 21.4% in spite of the reduction in temperature. The transmittance values for the highest liquid loading flame are still much higher than those observed for comparable acetylene and toluene flames. Therefore, the X_R is much lower than that for the heavily sooty acetylene and toluene flames. It is apparent that the relatively high momentum of the liquid jet flames causes the soot formation process to be incomplete leading to higher flame transmittance and lower radiation heat loss. The relatively high values of measured temperatures suggest that the

reduced radiant loads are not due to incompleteness of combustion.

For engine combustion applications, where soot loading and heat transfer to the wall are to be reduced, the present work suggests a method of control. However, within the present limited objectives of simulating crude oil well blowout flames, this possibility could not be explored further.

CONCLUSIONS

The following conclusions can be drawn from the present study:

(1) The effervescent atomizer-burner leads to efficient combustion of crude oil/methane/hydrogen flames with very high liquid loading.

(2) The measurements of flame height showed systematic effects of liquid loading and atomization quality. The flame heights increased with increasing heat release rates and decreasing methane to liquid mass flow rate due to the longer distance needed for evaporation of the drops.

(3) The measurements of radiant heat loss fractions were unexpectedly low but can be explained by the effects of the high exit momentum on soot formation. Based on the emission temperature measurements, incompleteness of combustion did not play a role in the reduced radiant fractions.

(4) Study of additional operating conditions, particularly those with increased residence time are needed to obtain generalized global properties for crude oil/methane flames.

ACKNOWLEDGEMENTS

This study was partially supported by the National Institute of Standards and Technology, Building and Fire Research Laboratory

under Grant No. 60NANB1D1172 with Dr. D. D. Evans serving as NIST Scientific Officer. The work regarding oil well fires at NIST is supported by the Mineral Management Service of the US Department of Interior with Mr. Charles Smith and Mr. Ed Tennyson serving as Program Managers.

REFERENCES

Dalzell W. H. and Sarofim A. F., 1969, "Optical Constants of Soot and Their Application to Heat Flux Calculations," ASME Journal of Heat Transfer, Vol. 91, pp. 100-104.

Evans D. D. and Pfenning D., 1985, "Water Sprays Suppress Gas-Well Blowout Fires," Oil and Gas Journal, Vol. 83, No. 17, pp. 80-86.
Faeth G. M., 1987, "Mixing, Transport and Combustion in Sprays," Prog. Energy Combust. Sci., Vol. 13, pp. 293-345.

Faeth G. M., Gore J. P., Chuech S. G. and Jeng S. M., 1989, "Radiation from Turbulent Diffusion Flames," Annual Review of Numerical Fluid Mechanics and Heat Transfer, Vol. 2, Chapter 1, C. L. Tien and T. C. Chawla, Eds., Hemisphere, pp. 1-38.

Gore J. P. and Evans D. D., 1991, "Technology Assessment and Research Program of the Offshore Mineral Operations," OCS Study MMS 91-0057, J. B. Gregory, C. E. Smith, and E. J. Tennyson, Eds., United States Department of Interior, Washington D.C.

Gore J. P., Klassen M., Hamins A., and Kashiwagi T., (1991), Fuel Property Effects on Burning Rate and Radiative Transfer from Liquid Pool Flames, Fire Safety Science Proceedings of The Third International Symposium, (G. Cox and B. Langford, eds.), Elsevier Science Publishers Ltd., London, pp. 395-404.

Gore J. P., Skinner S. M., Stroup, D. W., Madrzykowski D. and Evans D. D., 1989, "Structure and Radiation Properties of Large Two Phase Flames," Heat Transfer in Combustion Systems, ASME HTD Vol. 122, Ashgriz N, Quintiere J. G., Semerjian H. G. and Slezak S. E., Eds., pp. 77-86.

Hustad H. and Sonju O. K., 1986, "Radiation and Size Scaling of Large Gas and Gas/Oil Diffusion Flames," Dynamics of Reactive Systems Part I: Flames and Configurations, J. R. Bowen and R. I. Soloukhin, Eds., Vol. 105, Progress in Astronautics and Aeronautics Series, AIAA, New York, pp. 365-387.

Lund M. T., Sojka P. E., Lefebvre A. H. and Gosselin P. G., 1993, "Effervescent Atomization at Low Mass Flowrates. Part I: The Influence of Surface Tension," Atomization and Sprays, accepted.

Lund M. T., Jian C. Q., Sojka P. E. and Gore J. P., 1993, " The

Influence of Atomizing Gas Molecular Weight on Effervescent Atomizers Performance," Atomization and Sprays, submitted.

Sivathanu Y. R., 1990, "Soot and Radiation Properties of Buoyant Turbulent Diffusion Flames," Ph. D. Thesis, The University of Michigan, Ann Arbor, MI.

Sivathanu Y. R., Gore J. P. and Dolinar J., 1991, " Transient Scalar Properties of Strongly Radiating Jet Flames," Combust. Sci. and Tech., Vol. 76, pp. 45-66.

Sivathanu Y. R., Gore J. P., J. M. Janssen, and D. W. Senser, 1993, "A Study of Specific Absorption Coefficients of Soot Particles in Laminar Flat Flames," ASME Journal of Heat Transfer, in press.

Sivathanu Y. R. and Gore J. P., 1993, "Total Radiative Heat Loss in Jet Flames from Single Point Radiative Flux Measurements," Comb. Flame, revised.

LIST OF FIGURES

LIST OF TABLES

TABLE OF OPERATING CONDITIONS

Test Case	$\dot{m}_{OIL}$ (mg/s)	$\dot{m}_{CH_4}$ (mg/s)	$Re_{d = 4.76\ mm}$	$Re_{d = 1.87\ mm}$	Q_f (kW)	X_R (%)
1.	135	27.0	3.8×10^3	1.7×10^5	9.2	11.4
2.	234	32.8	5.5×10^3	2.2×10^5	14.2	10.2
3.	238	23.8	4.9×10^3	1.5×10^5	13.5	15.5
4.	250	25.0	5.1×10^3	1.7×10^5	14.0	14.0
5.	260	13.0	4.8×10^3	8.7×10^4	13.9	21.4
6.	328	16.4	5.4×10^3	1.1×10^5	17.0	20.7
7.	360	18.0	5.7×10^3	1.2×10^5	18.5	20.6
8.*	400	20.0	6.9×10^3	1.3×10^5	21.0	19.5

*HIGHER HYDROGEN FLOW RATE

$$Re_d = \frac{\rho_{TP}\, V_{TP}\, d}{\mu_{TP}}$$

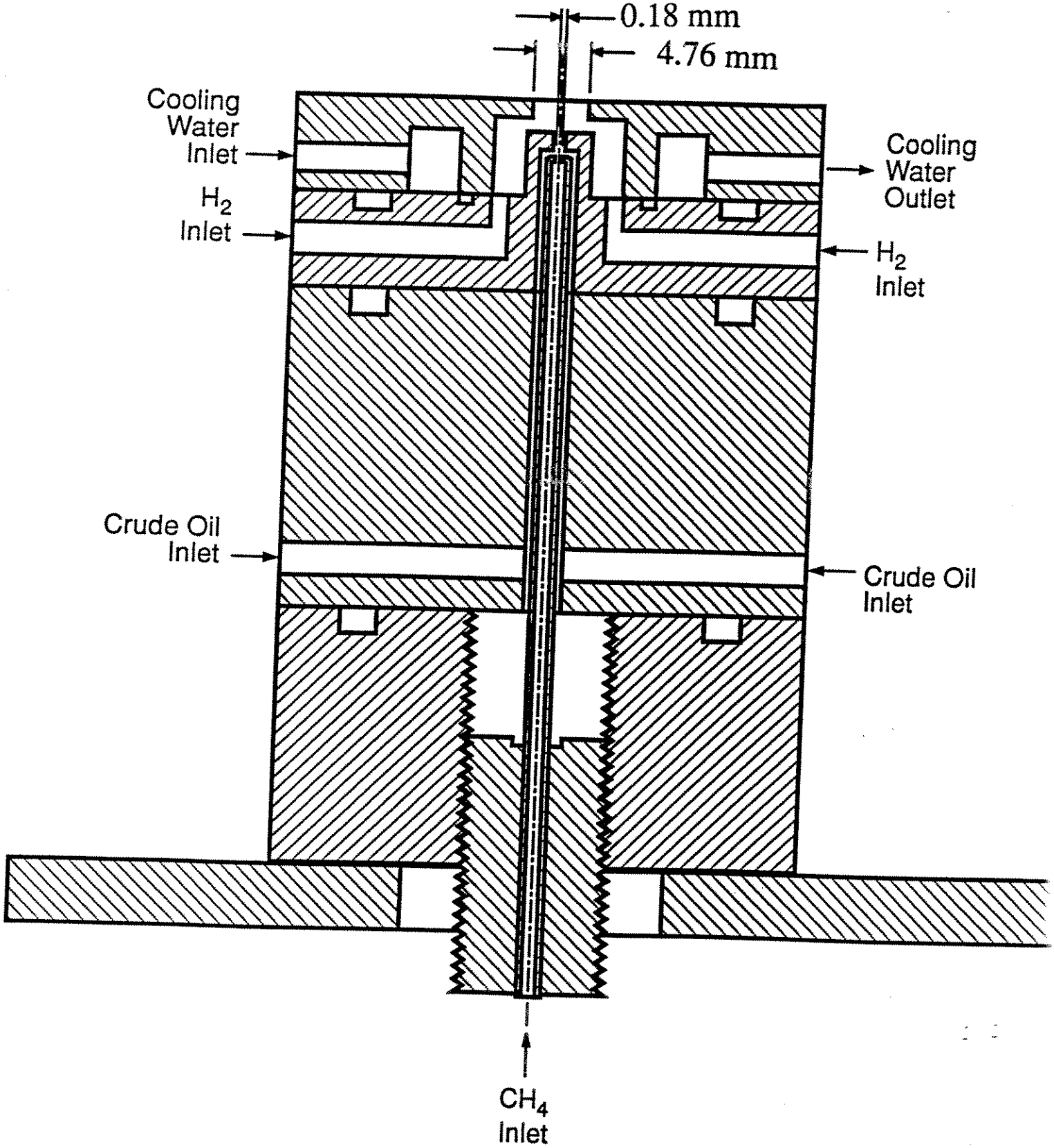

Fig. 1 Dutta et al.

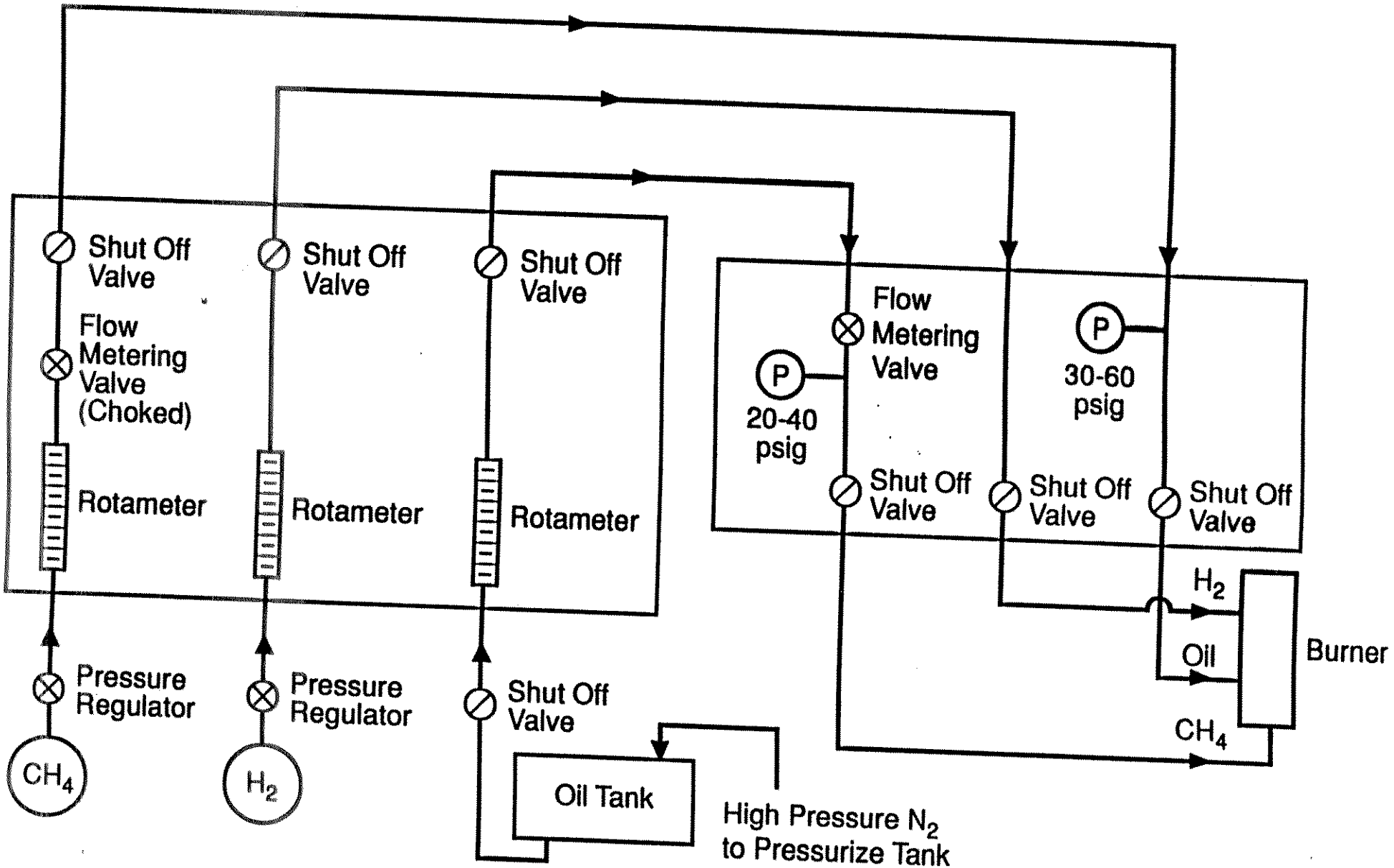

Fig. 2 Dutta et al.

Schematic of Flow System

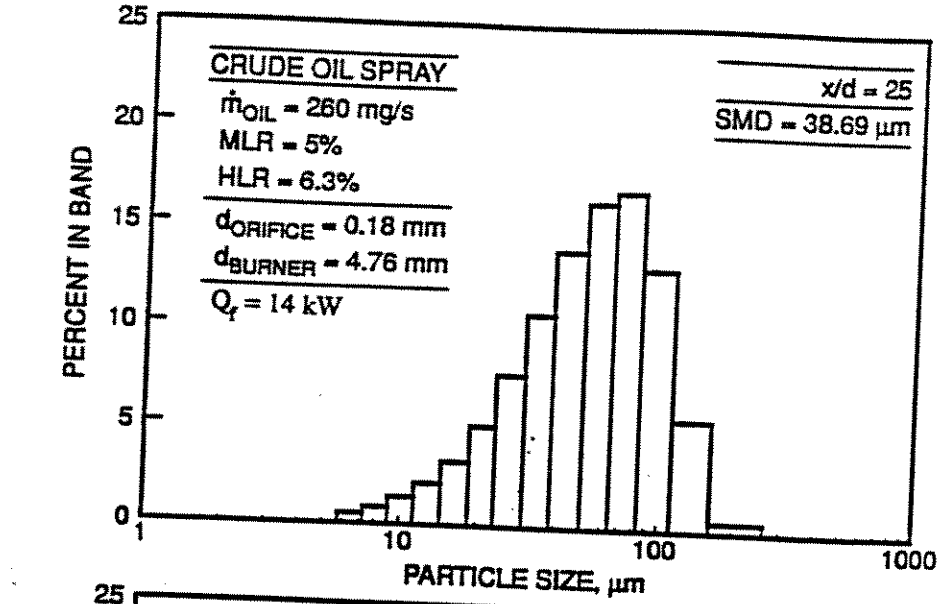

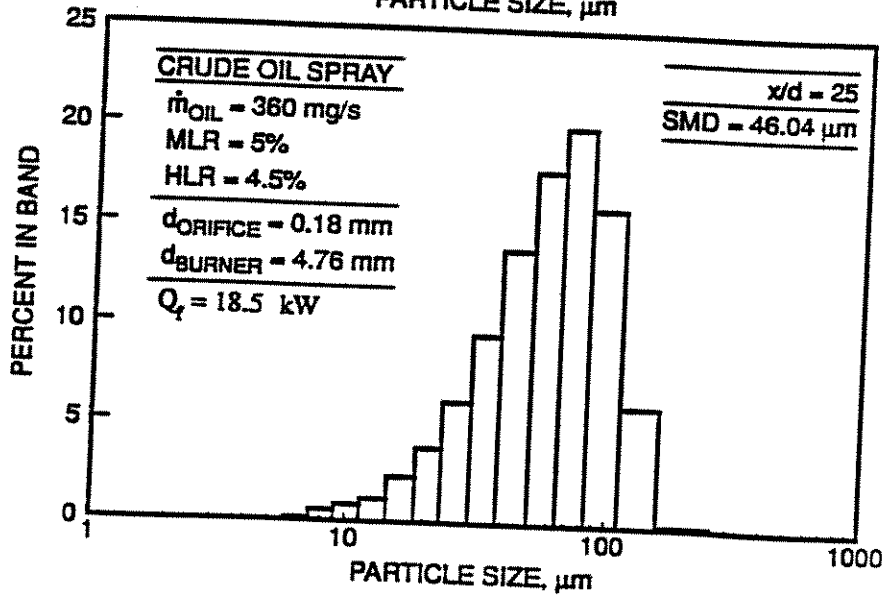

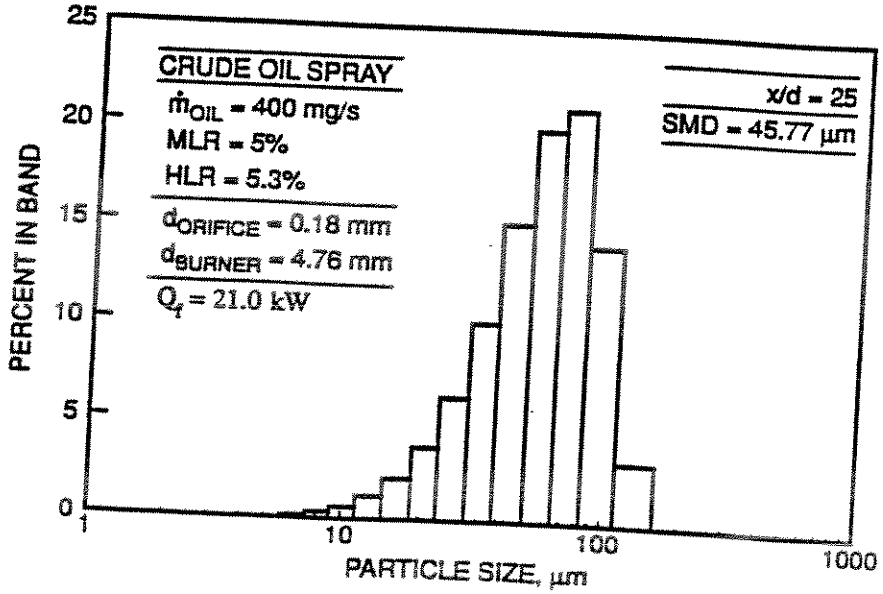

Fig. 3 Dutta et al

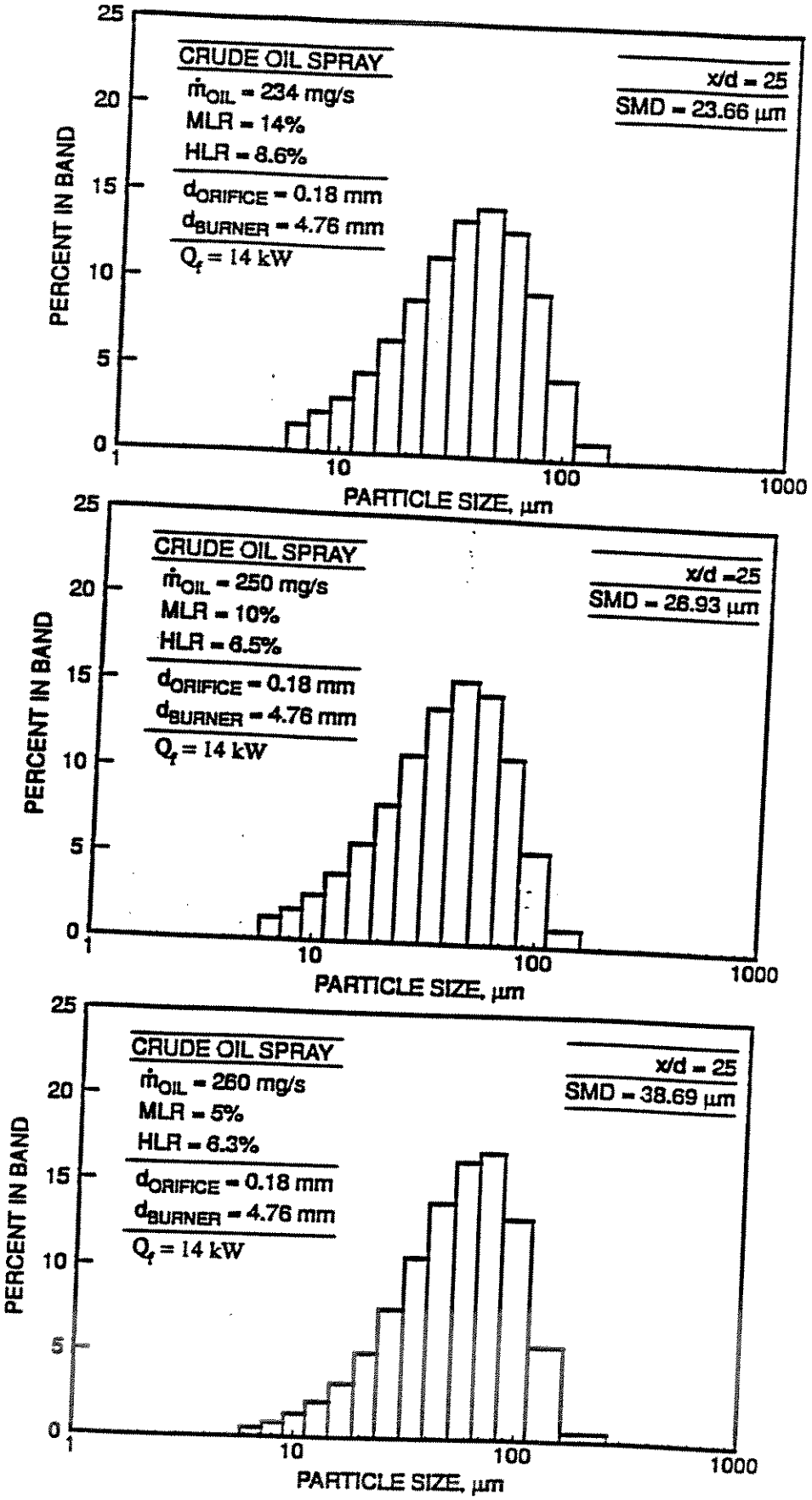

Fig. 4 Dutta et al.

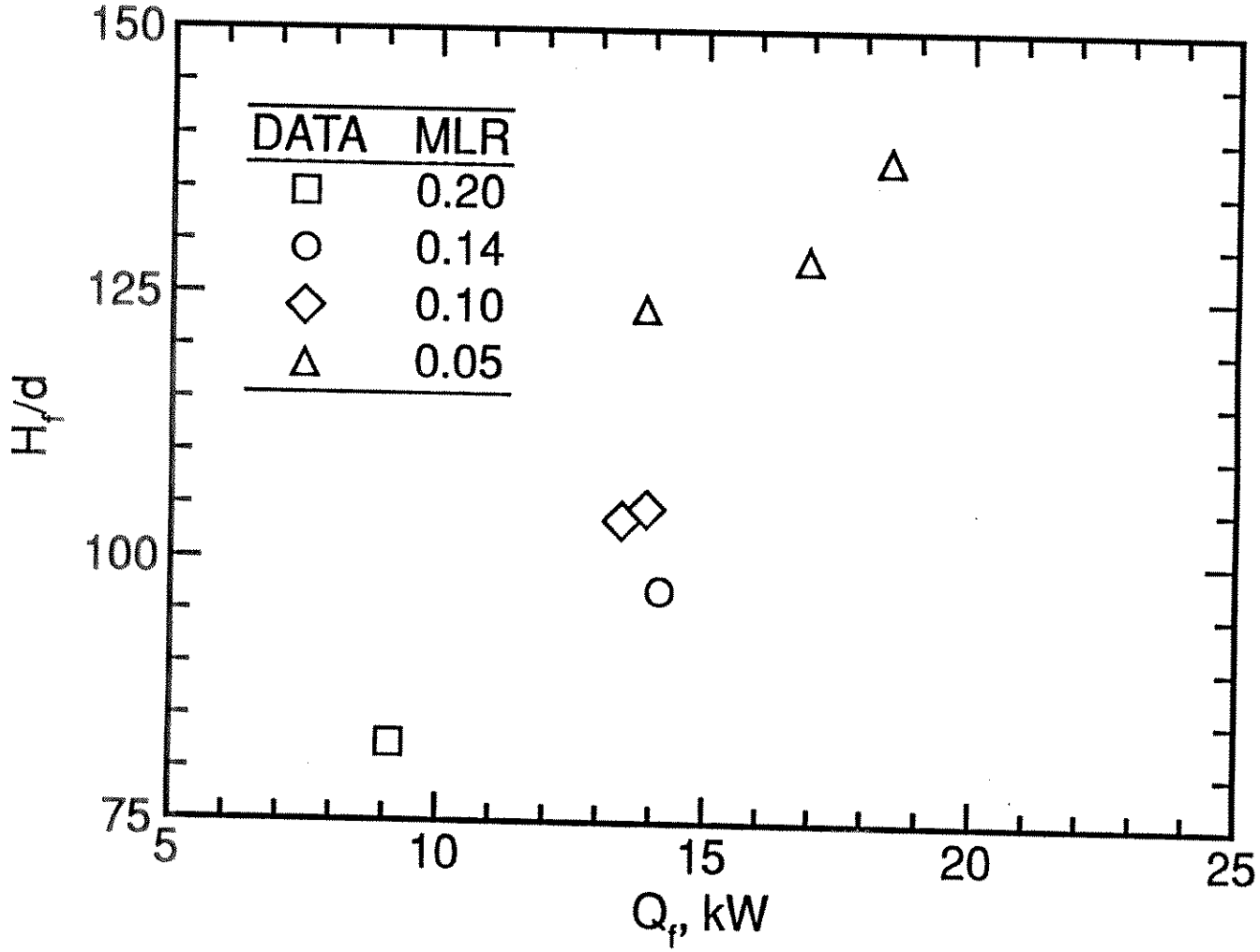

Fig. 5 Dutta et al.

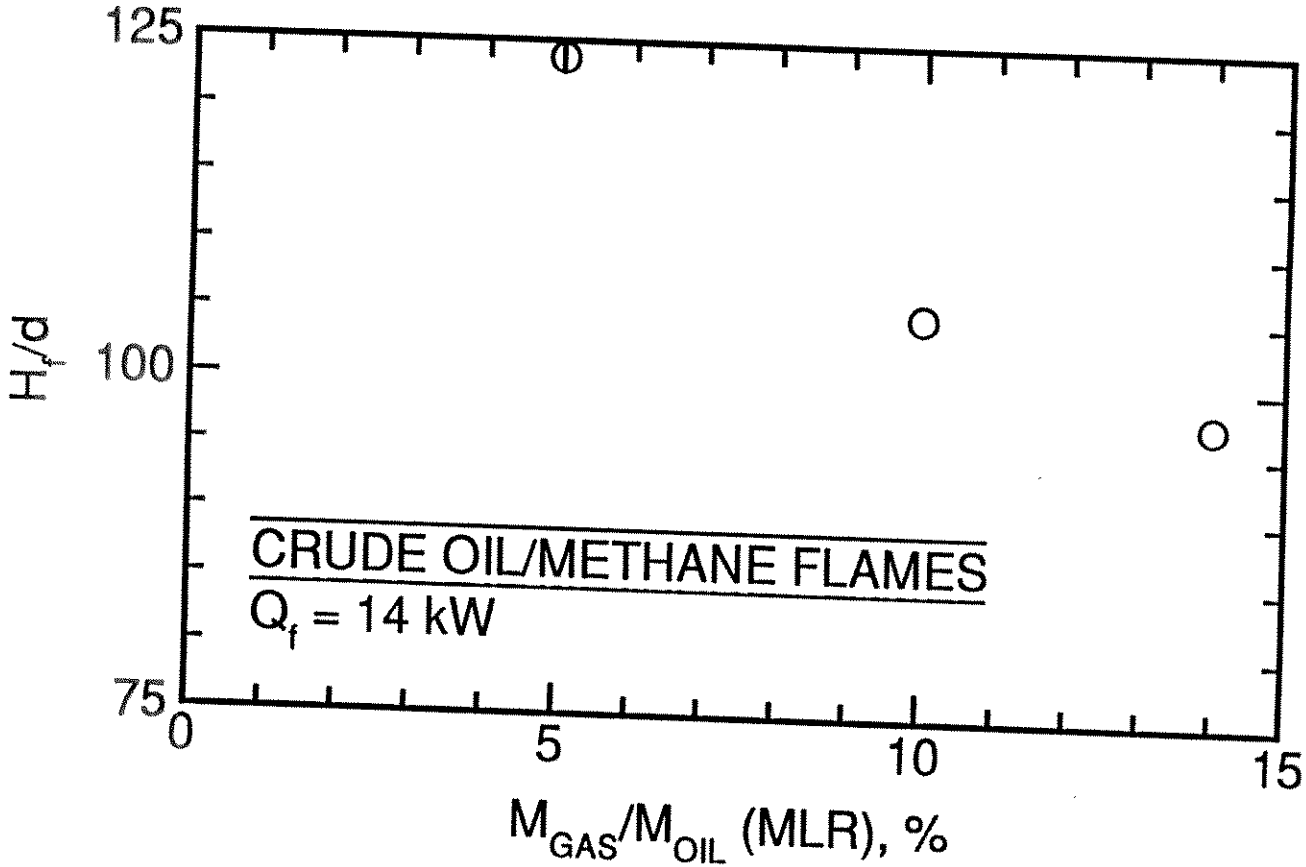

Fig 6 Dutta et al.

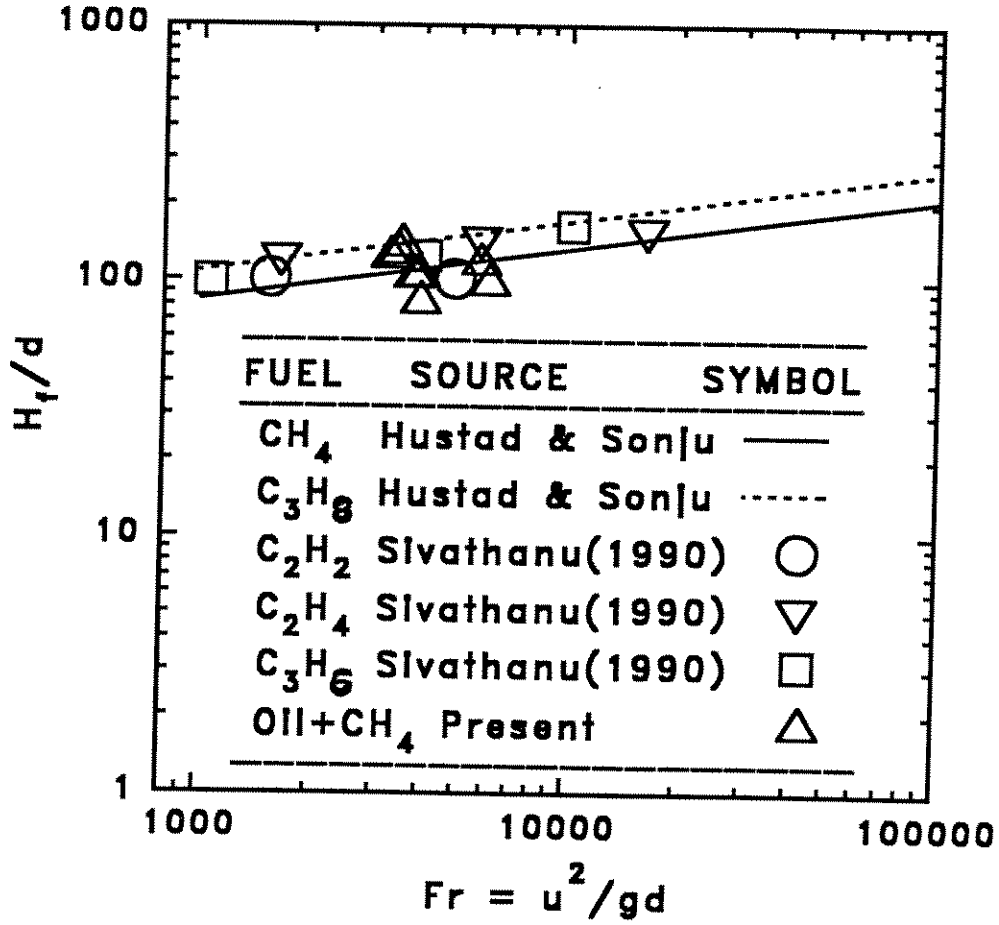

Fig. 7 Dutta et al.

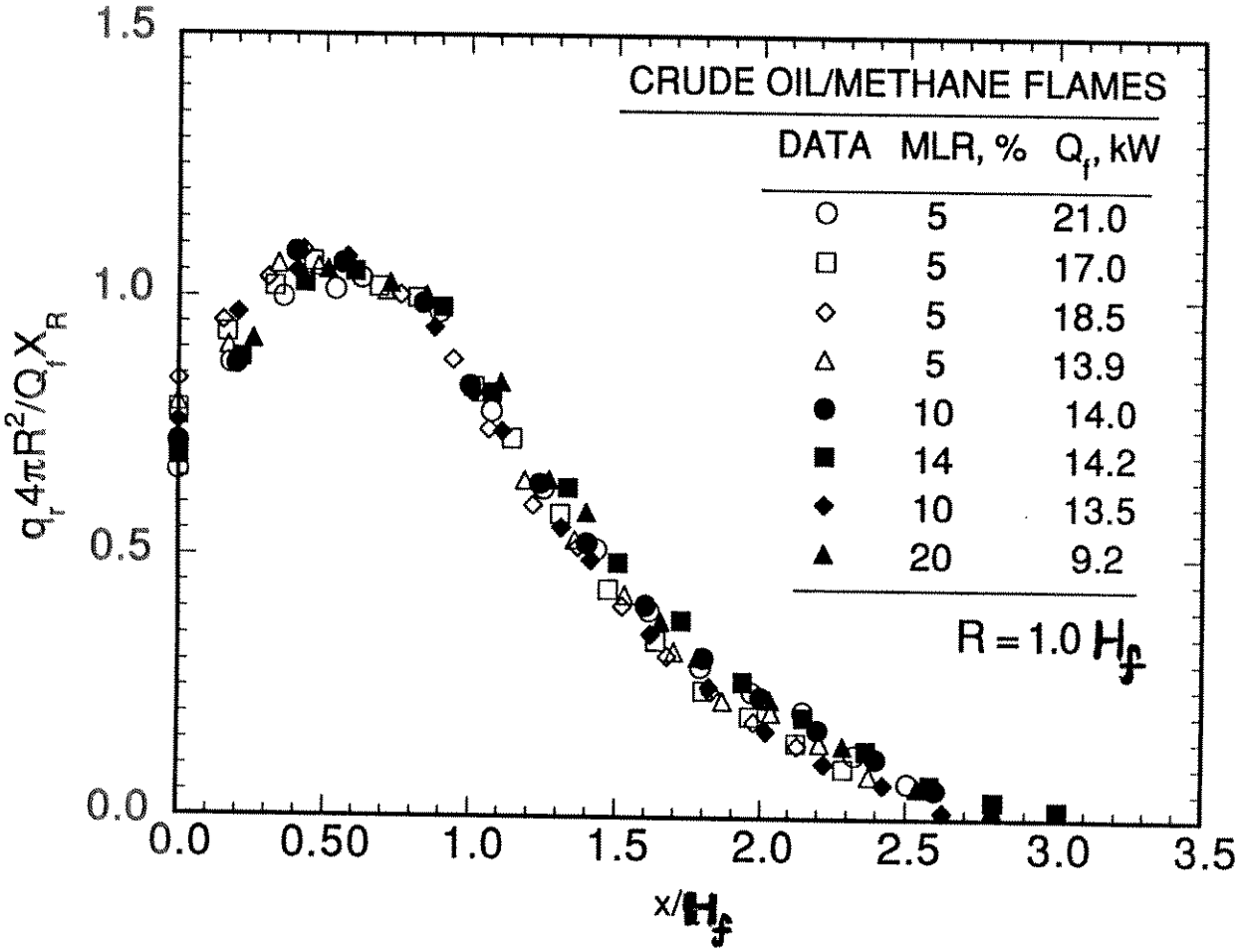

Fig. 8 Dutta et al.

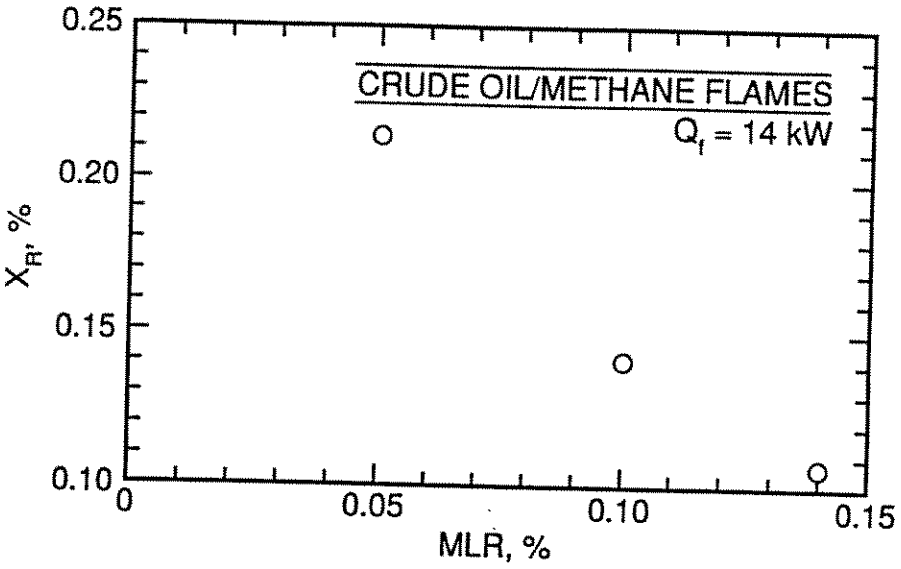

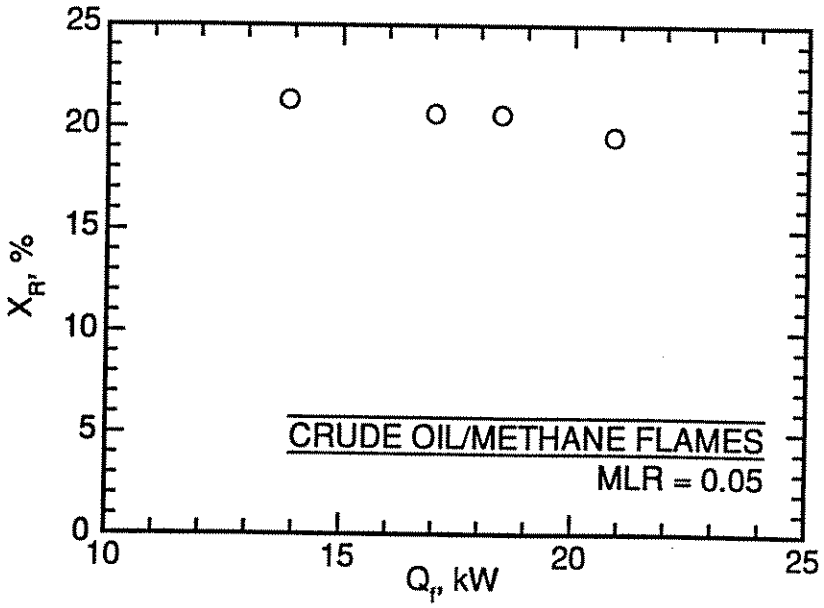

Fig. 9 Dutta et al.

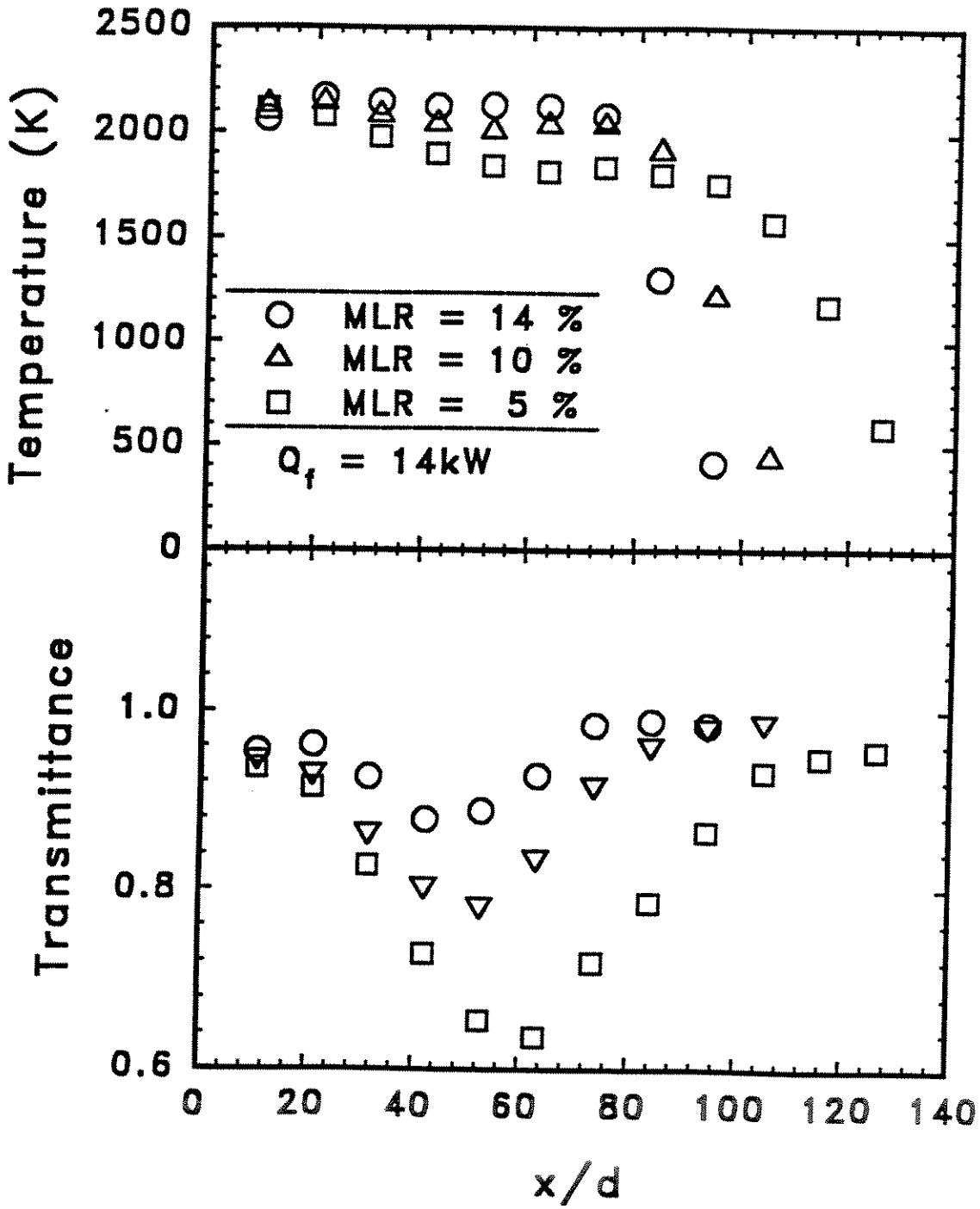

Fig. 10 Dutta et al.